ELSEVIER

International Journal of Heat and Fluid Flow 20 (1999) 545–551

International Journal of HEAT AND FLUID FLOW

www.elsevier.com/locate/ijhff

# Measurements of a diesel spray with a normal size nozzle and a large-scale model

Pekka Rantanen [a,*], Antti Valkonen [a], Andreas Cronhjort [b]

[a] *Helsinki University of Technology, P.O. Box 4300, Fin-02015 Hut, Finland*
[b] *Royal Institute of Technology, 100 44 Stockholm, Sweden*

**Abstract**

Advantages of the large-scale modeling of diesel sprays based on dimensional analysis were studied. Measurements of the spray tip penetration, spray angle, droplet size and velocity in a diesel spray have been made with a small nozzle and a large-scale model of the same nozzle. Measurements were made with image analysis, diffraction drop size analyzer and laser Doppler anemometer. Results show that scaling might give us new possibilities to research diesel sprays. 

*Keywords:* Diesel fuel spray; Scaled model; Drop size

**Notation**

| | |
|---|---|
| $D$ | nozzle hole diameter |
| $d$ | droplet diameter |
| $K$ | cavitation number |
| Oh | Ohnesorge number |
| $P$ | pressure |
| Re | Reynolds number |
| $T$ | temperature |
| $t$ | time |
| $S$ | spray tip penetration |
| $\eta$ | viscosity |
| $\rho$ | density |
| $\sigma$ | surface tension |
| *Subscripts* | |
| f | fuel |
| g | gas |
| i | injection |
| *Superscript* | |
| * | dimensionless |

## 1. Introduction

Diesel sprays are a challenging subject for measurements. In measurements made with a test rig for Wartsila Vasa 46 engine, Rantanen et al. (1994), it was realized that due to high concentration it is difficult or impossible to measure the droplet size distribution at the inner parts of the spray. The most obvious solution to the problem is to cut away a part of the spray, but high velocities in the spray make this difficult. Even so, some estimates of the droplet size were measured with this technique.

According to a study done by Paloposki (1995) it was shown that experiments made with a large-scale model give new possibilities to overcome the difficulties in measurements. With a nozzle larger than the natural size, the velocity of the spray decreases and droplet size increases. This facilitates the use of the measurement equipment as the spatial and temporal resolution of the measurements increases. For LDV and PDA measurements this is a great help in avoiding multiple droplets in the measurement volume due to decrease in the number concentration of the droplets. Most of all the imaging of droplets and the image analysis of droplet sizes will be easier as the velocity of the spray decreases. Longer exposure times can be used and it is easier to implement cutter techniques. In addition to this, droplet size increases to the range of imaging techniques and there is an easier range for the measurement of scattering angles, as longer focal lengths and measurement distances can be used.

Large-scale modeling has been used successfully in other areas of spray research. Walzel (1982) used large-scale models in spray formation studies and small-scale models of black liquor nozzles of recovery boilers and heavy oil nozzles of blast furnaces have been used in splash plate nozzle studies. Large-scale models have been used for the research of the fuel flow inside the diesel nozzle, the sack and the hole by Soteriou et al. (1995), but not for spray studies.

Many benefits can be achieved directly with experiments made with scaled models. In addition to this, experiments with scaled models can give us valuable information about spray formation and the atomization mechanism even if scaling laws do not describe the behavior of diesel sprays.

* Corresponding author. E-mail: pekka.rantanen@hut.fi

0142-727X/99/$ – see front matter 
PII: S0142-727X(99)00046-6

## 2. Scaling

Large-scale modeling of diesel fuel injection is based on dimensional analysis made by Paloposki (1995). Nozzles are geometrically similar and the diameter of the nozzle hole represents the geometrical scale. In addition to the geometry, the independent variables which were considered to be essential for the spray formation were the pressure difference at the nozzle and injection time and fluid properties. The properties required were density, viscosity and surface tension of the fuel and density, viscosity and pressure of the gas. The effect of the gas pressure and cavitation was studied separately. Dimensionless variables which should be kept the same in the large-scale model as in the real case, were:

$$\text{Reynolds number} \quad \mathrm{Re} = \frac{D}{\eta_\mathrm{f}}\sqrt{\rho_\mathrm{f}\Delta p}, \tag{1}$$

$$\text{Ohnesorge number} \quad \mathrm{Oh} = \frac{\eta_\mathrm{f}}{\sqrt{D\rho_\mathrm{f}\sigma}}, \tag{2}$$

$$\text{Dimensionless injection time} \quad t^* = \frac{t}{D}\sqrt{\frac{\Delta p}{\rho_\mathrm{f}}}, \tag{3}$$

$$\text{Density ratio} \quad \rho^* = \frac{\rho_\mathrm{f}}{\rho_\mathrm{g}}, \tag{4}$$

$$\text{Viscosity ratio} \quad \eta^* = \frac{\eta_\mathrm{f}}{\eta_\mathrm{g}}, \tag{5}$$

$$\text{Cavitation number} \quad K = \frac{\Delta p}{p_\mathrm{g}}. \tag{6}$$

The dependent variables which we are interested in are as follows:

$$\text{Dimensionless droplet size} \quad d^* = \frac{d}{D}, \tag{7}$$

$$\text{Dimensionless spray tip penetration} \quad S^* = \frac{S}{D}, \tag{8}$$

$$\text{Spray angle} \quad \Theta = \Theta, \tag{9}$$

$$\text{Dimensionless droplet concentration} \quad C_N^* = C_N^* D^3, \tag{10}$$

$$\text{Dimensionless injection quantity} \quad \Delta m^* = \frac{\Delta m}{\rho_\mathrm{f} D^3}. \tag{11}$$

For the scaled experiment we have nine variables, which should be chosen in a way that independent dimensionless variables in Eqs. (1)–(6) are constant. For practical reasons experiments were made with hydrocarbon liquids and in nitrogen atmosphere. This restricts our options. Firstly, density and surface tension of hydrocarbons varies in such a small range that they can be considered to be constant. Secondly, viscosity of the gas is only a function of the temperature. In experiments made at ambient temperature we cannot change viscosity. Thirdly, density and pressure of the gas are not independent when gas is fixed. This leaves us five variables to satisfy six equations. Due to the restrictions all the dimensionless variables can be kept constant only at some special cases.

However, scaling gives us the possibility to make test at room temperature where the cavitation number is same as in a real engine. Variables must be chosen for a large-scale test in a way that only viscosity ratio is higher than in the real engine. To achieve this the geometrical scaling must be

$$\psi_D = \frac{p_\mathrm{g}}{p'_\mathrm{g}} = \frac{T_\mathrm{g} M'_\mathrm{g}}{T'_\mathrm{g} M_\mathrm{g}}. \tag{12}$$

Since the density of the gas must be same as in normal scale, the gas pressure in the measurement chamber at large scale is fixed at ambient temperature by the selection of the gas. In modeling of fuel injection of a real engine this gives scaling factor of 3–6 depending on the engine and molecular weight of the gas used in the experiments.

In a small scale, test variables can be chosen in a way that only the cavitation number is higher than in the real engine. The geometrical scaling must be then

$$\psi_D = \left(\frac{\eta'_\mathrm{g}}{\eta_\mathrm{g}}\right)^2, \tag{13}$$

Viscosity is fixed by the selection of the gas and the temperature. Typically this means scaling 1:2 to 1:2.5 at ambient temperatures.

The diameter of the nozzle hole, $D$, presents the geometrical scale of the model, $\psi_D$. Scale of the other dimensional variables as a function of geometrical scale is presented in the following table.

| | Scaling factor | Example |
|---|---|---|
| *Independent variables* | | |
| Geometrical scale | $\psi_D = \psi_D$ | 4 |
| Pressure | $\psi_{\Delta p} = 1/\psi_D$ | 1/4 |
| Time | $\psi_{\Delta t} = \psi_D^{3/2}$ | 8 |
| Fuel and gas density | $\psi_{\rho_\mathrm{f}} = 1$ | 1 |
| Fuel and gas viscosity | $\psi_{\eta_\mathrm{f}} = \sqrt{\psi_D}$ | 2 |
| Surface tension | $\psi_\sigma = 1$ | 1 |
| *Dependent variables* | | |
| Droplet size | $\psi_d = \psi_D$ | 4 |
| Spray tip penetration | $\psi_S = \psi_D$ | 4 |
| Spray angle | $\psi_\Theta = 1$ | 1 |
| Droplet concentration | $\psi_{C_N} = 1/\psi_D^3$ | 1/64 |
| Injected mass | $\psi_m = \psi_D^3$ | 64 |

In a large-scale test, droplets will be larger than in the real engine due to lower injection pressure and larger nozzle. Moreover, the velocity of the droplets will be lower as in the real engine. Thus it is expected that measurement of the droplets will be easier.

One of the objectives for the large-scale modeling was to make measurement of the droplet sizes easier. The main problem in the measurements with light scattering techniques is the high droplet concentration in the middle of the spray and subsequent high obscuration of the light passing through the spray. Obscuration is determined by equation

$$\mathrm{Ob} = 1 - I/I_0, \tag{14}$$

where $I_0$ is the intensity of the incident beam and $I$ the transmitted intensity. The extinction cross efficiency is constant for Fraunhofer diffraction at this size range. Therefore, extinction of the light is directly proportional to the ratio of projected area of the droplets to the beam cross section. This ratio remains constant at the scaling. So, we do not expect any change in the obscuration. However, lower obscuration is achieved with the large-scale model using cutters. Transmitted intensity is proportional to the beam length inside the spray according to Bouguer's law

$$\ln(I/I_0) \propto L. \tag{15}$$

With the cutters the active beam length, $L$, will be constant. Obscuration in the scaled model, $\mathrm{Ob}_\phi$, is

$$\mathrm{Ob}_\phi = 1 - (1 - \mathrm{Ob}_0)^{1/\phi_D}. \tag{16}$$

In a large-scale model decrease of obscuration will be significant and measurements with cutters are thus easier.

## 3. Equipment

The basis for the measurements was a nozzle with five holes from a Valmet 620 DS engine. The large-scale nozzle was based on the Wartsila Vasa 46 engine in which the dimensions are originally about 4 times the Valmet engine. This scaling factor also gives us the advantage that the cavitation number is the same in the real engine and on the large scale at room temperature in a nitrogen atmosphere. Large-scale measurements were made at Helsinki University of Technology with a test rig for the Vasa 46. Some changes in the springs of the injection valve and pump were made. Normal scale measurements were made at the Royal Institute of Technology with a test facility for small injectors, Hallberg and Ångström (1996). Parameters in the both measurements are presented in Table 1.

### 3.1. Normal-scale test rig

In the test rig, diesel fuel is injected into a pressurized vessel with optical access. The optical access is achieved by means of two glass windows, one for the light from the flash, the other for the camera. The injection vessel is equipped with pressure and temperature transducers to monitor the internal conditions. Electric heaters and solenoid valves are added to allow the computer to regulate the pressure and temperature in the vessel. It has turned out that the optical resolution of the system is very sensitive to diesel droplets on the windows, and therefore a special purge nozzle is included inside the vessel to blow away any diesel mist from the windows only a few milliseconds after the exposure of the picture.

The injector uses an internal hydraulic pressure booster and allows injection pressures up to 200 MPa to be used. The computer manages the entire system and thereby allows systematic photographic studies in predefined ambient conditions to be performed. The temperature in the vessel can be varied between 30°C and 100°C and the gas pressure between 0.1 and 5 MPa. The computer first adjusts temperatures and pressures in the system according to the predefined values. Then the injector is activated and the picture exposed. Between each picture the vessel is purged with hot air. As each picture is exposed, the computer stores the corresponding actual values for the regulated parameters together with the injection sequence.

### 3.2. Large-scale 4:1 test rig

The large-scale test rig is based on the test rig for the Vasa 46 engine with some modifications. The test rig consists of an injection bench, a measurement chamber and instrumentation. The injection bench consists of an electric motor driven by a frequency converter, flywheels, camshaft and injection pump with fuel and lubrication systems. The fuel is injected into a pressurized measurement chamber, which is equipped with windows for observations and measurements, as well as gas circulation and filtering. The instrumentation includes control measurements for oil, fuel and gas pressures and temperatures, and fast measurements for injection pressure, needle lift and timing.

For the large-scale tests, the injection pipe was changed to a longer one. The springs of the main flow valve and return valve in the injection pump were changed to correspond to lower pressures. The spring in the injection valve was changed as well to obtain a lower opening pressure of 6 Mpa. The pressure curves of the real engine and scaled rig are similar as can be seen from Fig. 1. Nozzle for the large-scale tests was from W46 engine with orifices drilled to the scaled size of 0.98 mm. Length to diameter ratio was 3.265 at both scales. Diameter of the sack was 4 mm at large scale and 1.025 mm at small scale.

In the large-scale test rig some of the measurements were made with a part of the spray deflected away to decrease the

Table 1
Dimensions for the large-scale tests (scale 4:1). Basis is Valmet 620 DS-diesel engine

| | | Engine | Ambient test rig | Model 4:1 |
|---|---|---|---|---|
| *Nozzle* | | | | |
| Number of the holes | | 5 | 5 | 5 |
| Diameter of the holes | $d$ (mm) | 0.245 | 0.245 | 0.98 |
| *Injection* | | | | |
| Pressure | $P_i$ (MPa) | 70 | 63 | 18 |
| Pressure difference | $\Delta P$ (MPa) | 59.5 | 60 | 15 |
| Injection duration | $\Delta t$ (ms) | 1.4 | 1.2 | 7 |
| *Fuel properties* | | | | |
| Density | $\rho_f$ (kg/m$^3$) | 837 | 848 | 847 |
| Viscosity | $\eta_f$ (kg/m s) | $2.6 \times 10^{-3}$ | $2.87 \times 10^{-3}$ | $5.55 \times 10^{-3}$ |
| Surface tension | $\sigma$ (mN/m) | 30 | 30 | 30 |
| *Gas in the cylinder* | | | | |
| Pressure | $P_g$ (MPa) | 10.5 | 3.00 | 3.00 |
| Temperature | $T_g$ (°C) | 930 | 20 | 20 |
| Density | $\rho_g$ (kg/m$^3$) | 30.5 | 34.5 | 34.5 |
| Viscosity | $\eta_g$ (kg/m s) | $48 \times 10^{-6}$ | $18 \times 10^{-6}$ | $18 \times 10^{-6}$ |
| *Dimensionless variables* | | | | |
| Reynolds number | Re | 21 000 | 19 256 | 19 900 |
| Ohnesorge number | Oh | 0.0331 | 0.0364 | 0.0352 |
| Injection duration | $\Delta t^*$ | 1520 | 1303 | 951 |
| Density ratio | $\rho^*$ | 27.4 | 24.6 | 24.6 |
| Viscosity ratio | $\eta^*$ | 54.2 | 160 | 308 |
| Cavitation number | $K$ | 5.67 | 20 | 5 |

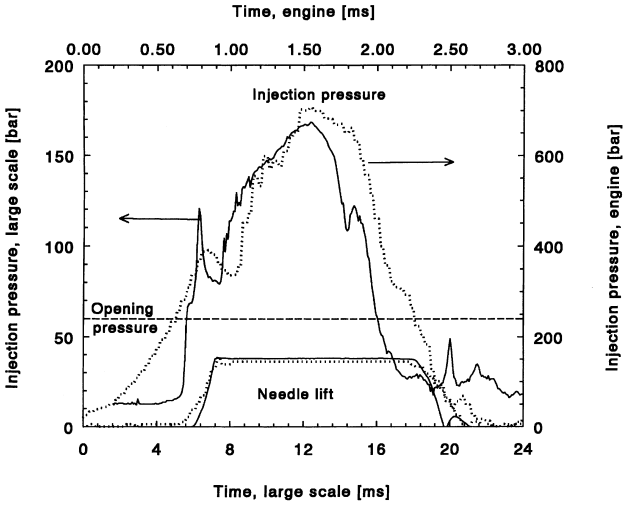


Fig. 1. Injection pressure curves of the real engine and the scaled model.

extinction of light. This was done with cutter blades inserted just in front of the measurement volume. Cutters are represented in Fig. 2.

## 4. Results

### 4.1. Spray angle

The spray tip penetration and spray angles were measured from images taken with a CCD camera. A stroboscope with a flash duration of 1 μs was used for background illumination. The stroboscope was triggered after a preset delay by the signal coming from the needle lift sensor and the camera was triggered from the flash by a photodiode, Fig. 3.

Scatter in the spray angles was fairly high. The opening angle was analyzed from 20 images at each measurement point. The standard deviation was 5%. Analysis was based on subjective estimates of the mean edges of the spray. Accuracy of the measurement of the spray angle was 1.5°. The spray angle was 20° in the large-scale model with a gas density of 23 kg/m$^3$ and an injection pressure difference of 100 bar. In the normal scale test in corresponding conditions, the spray angle was 23°. The spray was broader in the normal-scale test rig. This might be a result of the fact that the cavitation number in the ambient test rig was higher than in the large-scale rig. This means that in the real engine spray angles are lower than those measured in the ambient test rig, where cavitation is more intense.

### 4.2. Spray tip penetration

In the measurements made before, Rantanen et al. (1994) it has been observed that the correlation proposed by Hiroyasu and Arai (1990) represents quite well the spray tip penetration. The correlation is presented by the equation

$$S = \begin{cases} 0.39\sqrt{\frac{2\Delta P}{\rho_f}}, & t < t_b, \\ 2.95\left(\frac{\Delta P}{\rho_g}\right)^{0.25} d^{0.5} t^{0.5}, & t > t_b, \end{cases} \tag{17}$$

where $t_b$ is the time for the breakup,

$$t_b = 28.65 \frac{\rho_l d}{\sqrt{\rho_g \Delta P}}. \tag{18}$$

As the correlation is dimensionally correct, it was expected that it would predict the spray tip penetration in the scaled model. With the large-scale model it was possible to measure the spray tip penetration at distances longer than 75 mm from the nozzle tip. At these distances, spray tip penetrations of the two test cases were the same within the measurement accuracy as can be seen in Fig. 4. The same figure shows spray tip penetrations calculated from Eq. (18) with an effective pressure difference of 320 bar (80 bar for the 4:1 model). Calculation and measurements gave the same penetration up to half of the injection period. From then on calculation gave higher penetrations than measured. Spray tip penetrations measured at both scales gave results which are then the same as in the real engine except for the influence of vaporization and burning of the droplets.

### 4.3. Droplet size

Droplet sizes were measured with image analysis in both test rigs and with a Malvern particle size analyzer in the large-scale model. In the normal-scale test rig, it was not possible to use the Malvern due to the construction of the windows. The

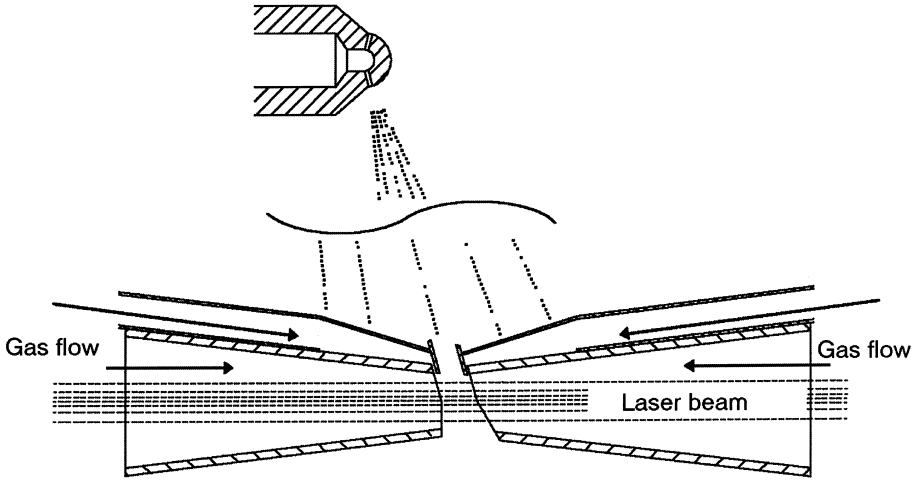


Fig. 2. Schematic representation of the cutters.

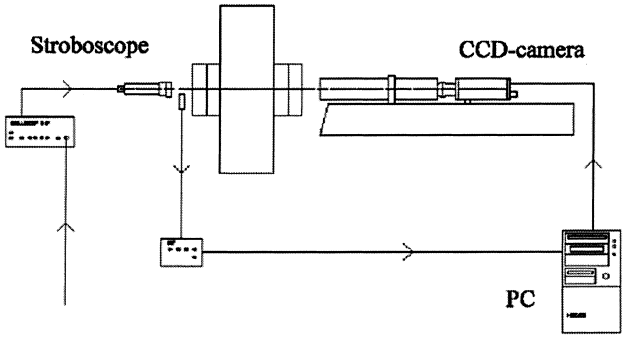


Fig. 3. Imaging equipment.

windows in that test rig were designed only for photographing of the spray.

With the Malvern, the droplet size at each measurement point was measured as the mean of 20 individual sprays with 30 s intervals. Droplet size was measured at distances of 0, 6, 11 and 16 mm from the centerline of the spray and 125 mm from the nozzle, as were all other measurements in the large-scale rig. Obscuration was high in the large-scale model without cutters, and droplet size could be measured reliably at the edges only. With cutters, obscuration decreased to an acceptable level even in the center of the spray as can be seen from Fig. 5.

Measurements made without cutters at the distances of 0 and 6 mm from the centerline of the spray are also reported in Figs. 6 and 7. Severe multiple scattering ruined the measurements as can be concluded from the high values of the

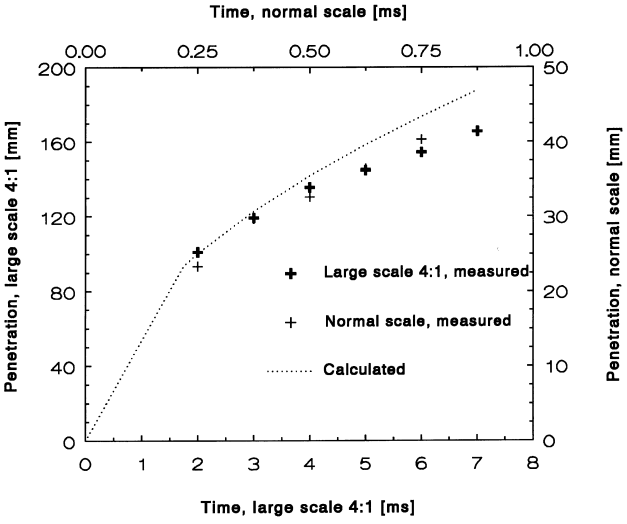


Fig. 4. Spray tip penetration in normal scale and 4:1 scaled test rig.

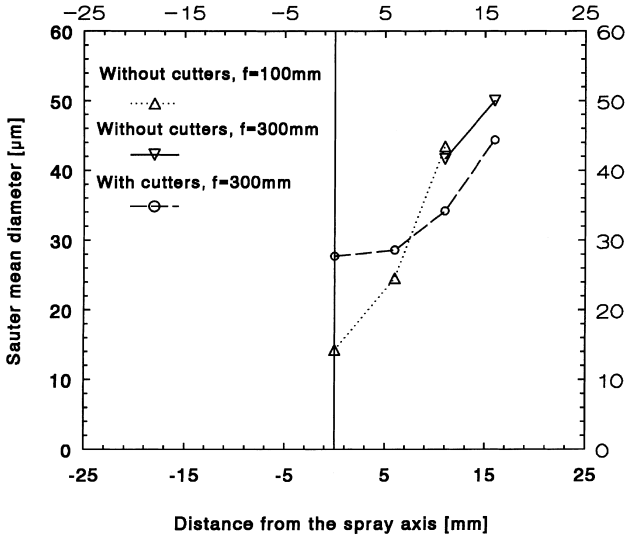


Fig. 6. Sauter mean diameters in the spray of the large-scale model, 35 rpm, gas density 23 kg/m$^3$.

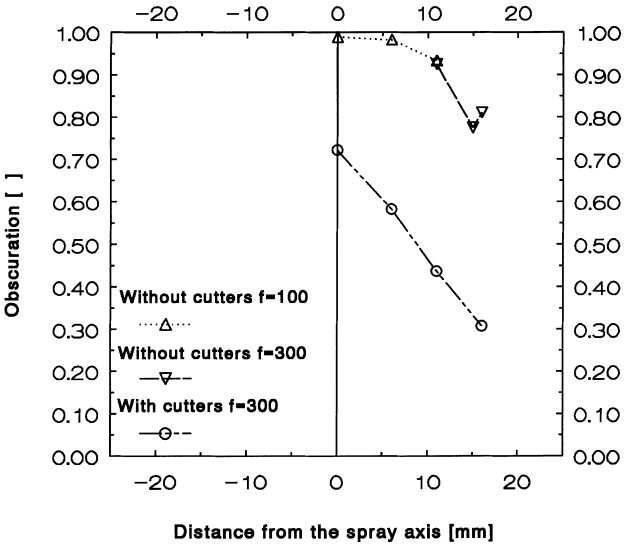


Fig. 5. Obscuration in the measurements with the large-scale model, 35 rpm, gas density 23 kg/m$^3$.

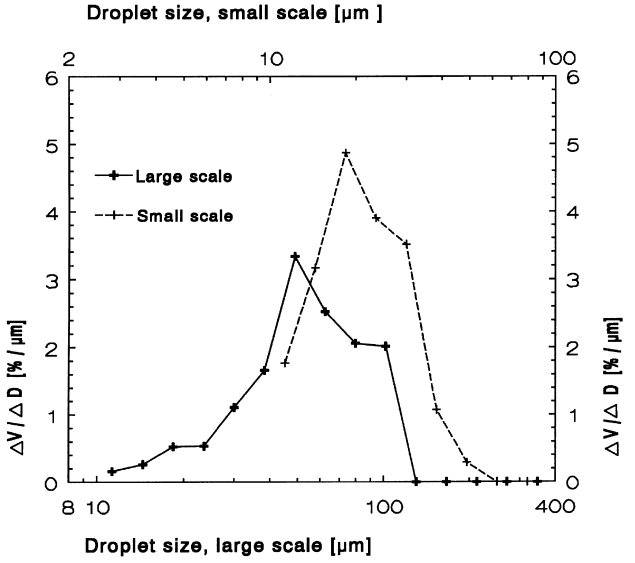


Fig. 7. Droplet size distributions measured with image analysis. Continuous line from the large-scale model, broken line from the normal-scale nozzle.

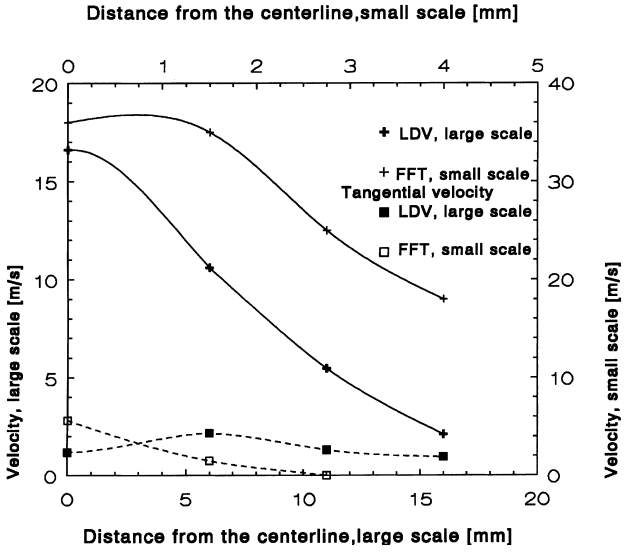


Fig. 8. Maximum velocities in large- and small-scale sprays.

obscuration. Droplet sizes and concentrations at these distances are not correct but are given only to give a view of the error associated with the multiple scattering. Sauter mean diameter was 50 μm at the outer part of the spray and 30 μm in the center of the spray, Fig. 6.

Drop size was analyzed from images taken with a fast shutter CCD-camera and a long distance microscope. The CCD-camera had a 1280 × 1024 pixel sensor and the shortest exposure time of the camera was 0.1 μs. The long distance microscope was designed for droplet imaging. The image area was 1.7 × 1.3–2.1 × 1.7 mm and the best resolution 3.5 μm. Analysis of the droplet sizes was made with a procedure developed for measurement of drop sizes of black liquor. In the analysis, the droplet size range was 10–500 μm. The lower limit was high for the small-scale measurements, as quite many of the droplets were smaller than 10 μm and Sauter mean diameters are not fully comparable. Droplet size was analyzed from 50 images at each measurement point. At the center of the spray, the quality of the images was not good enough to obtain a sufficient sample.

At the edge of the spray, 16 mm/4 mm from the spray axis in the large scale and normal scale accordingly, Sauter mean diameter was 58 μm / 21 μm. This gives a scale factor of 3 as the geometrical scale factor was actually 4. However, in the small scale the true Sauter mean diameter is smaller than 21 μm as we could not measure the smallest droplets. Fig. 7 presents the volume distribution of the droplets on the small and large scale. It can be seen that droplet size on the large scale is smaller than the scaling by about 20%.

This difference was not possible to explain with the difference in the scaling, which was in the viscosity ratio and the cavitation number. Cavitation number in the large-scale rig was lower than in the ambient test rig. This should lead to bigger droplet size, not smaller. Viscosity ratio is higher in the large-scale rig than in the ambient test rig and this should lead to bigger droplet size as well.

In the real engine this means that droplet sizes measured in the ambient test rig are too high and the real droplet size is

Fig. 9. Triple exposure image of a diesel spray at 31 mm from the nozzle and 4 mm from the centerline.

actually 20% lower. In this case that means droplet size of 15 μm at the edge of the spray.

### 4.4. Droplet velocity

Velocities in the small-scale spray were measured from multiple exposure images as in Fig. 8. Two-dimensional Fourier transform was calculated twice and image analysis used to find the most prominent wavelength. As the flash duration was only a few microseconds, only velocities over 20 m/s could be measured. Velocities in large-scale sprays were measured with a laser Doppler anemometer. Measured velocities are presented in Fig. 8. The velocity at the center of the spray was 36 m/s in the normal scale and 16.5 m/s on the large scale. This matches quite well the scaling factor, which is 2 for velocity. At the edges of the spray, scaling did not match as well as at the center but the velocity in the normal scale was higher there than on the large scale.

## 5. Conclusions

Measurements of properties of a diesel spray were made in two test rigs which were scaled 4:1 based on dimensional analysis (Fig. 9). The spray tip penetration was scaled accordingly. The spray angle was 15% higher in the normal scale. The droplet size was scaled up about 80% of the actual scaling. Droplet velocities were scaled correctly at the center of the spray. However, at the outer parts of the spray, the velocity was higher on the small scale than was expected according to scaling.

Differences between small and large scale were about the same as measurement accuracy. Some differences were observed and more thorough research should be done to verify whether the diesel sprays are suitable application for scaling. Although scaling might prove to be inaccurate in diesel sprays, it will give us valuable information about the break up and atomization mechanisms. According to these measurements, the essential mechanisms are of scalable nature.

## Acknowledgements

This work was supported by the LIEKKI 2 combustion research program of the Finnish Technology Development Centre, Wärtsilä-NSD, Neste and Sisu Diesel.

## References

Rantanen, P., Fontell, E., Paloposki, T., Turunen, R., Pitkänen, J., 1994. Fuel injection of a medium speed diesel engine, spray characterization. Helsinki University of Technology, Internal Combustion Engine Laboratory, Espoo, Report 66.

Paloposki, T., 1995. The use of dimensional analysis and model experiments in the research of fuel injection (in Finnish). Helsinki University of Technology, Laboratory of Energy Engineering and Environmental Protection, Espoo.

Walzel, P., 1982. Advantages and limits in large scale modeling of atomizers. ICLASS-82, Madison, Wisconsin, USA, 20–24 June, pp. 187–194.

Soteriou, C., Andrews, R., Smith, M., 1995. Direct injection diesel sprays and the effect of cavitation and hydraulic flip on atomization. SAE 950080.

Hallberg, M., Ångström, H.-E., 1996. Design of combustion bomb used for high resolution photography of diesel sprays. 12th Annual Conference of ILASS-Europe, Lund, Sweden, June 19–21.

Hiroyasu, H., Arai, M., 1990. Structures of fuel sprays in diesel engines. International Congress and Exposition, Detroit, Michigan, Feb 26–Mar 2, SAE 900475.